Supporting Information

Iwawaki et al. 10.1073/pnas.0903775106

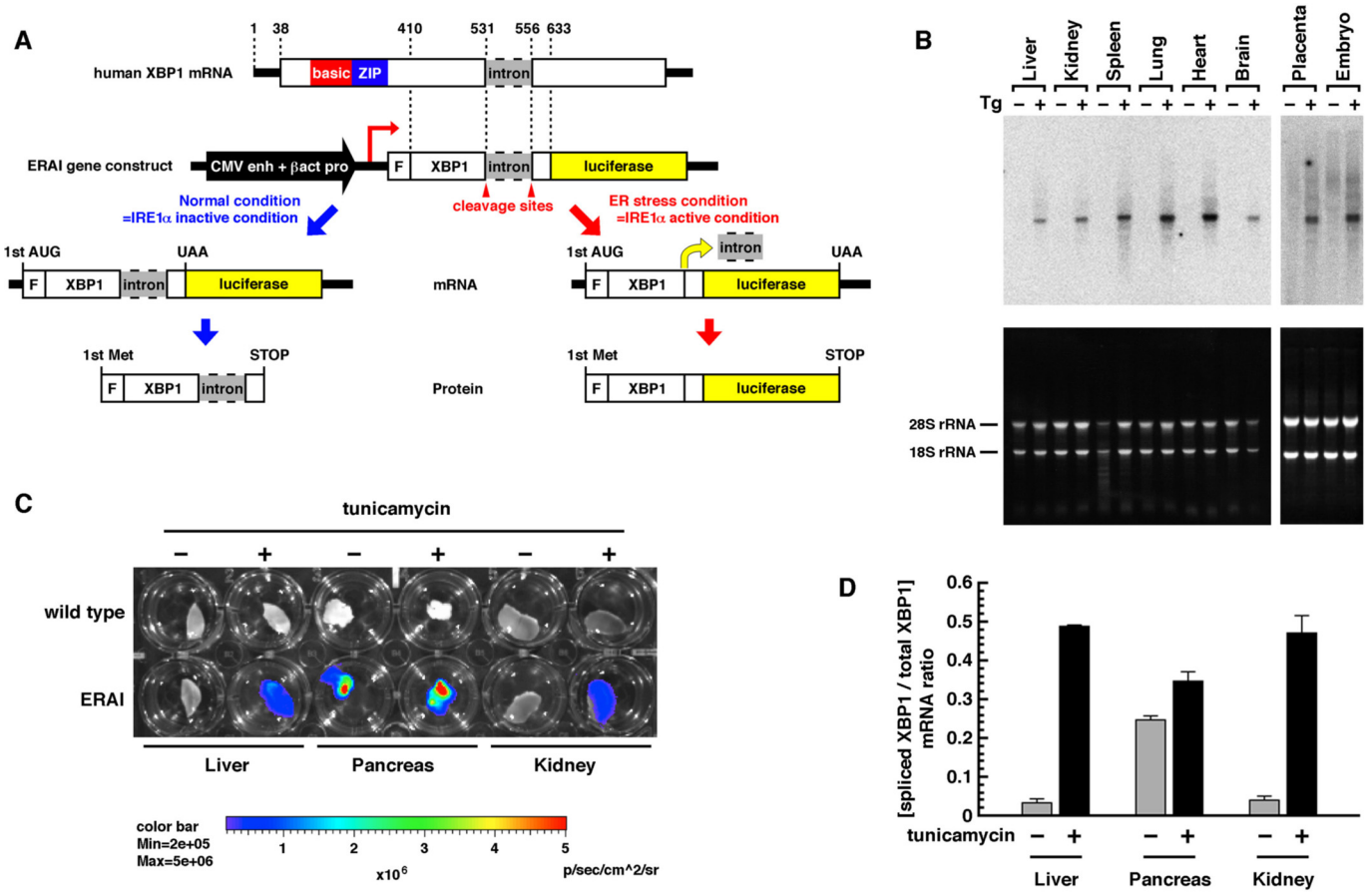

Fig. S1. Characterization of ERAI-LUC mice. (*A*) Schematic diagram of the ERAI-LUC system. The ERAI gene construct includes one part of the human XBP1 cDNA (410–633 nt). Basic (red) and ZIP (blue) indicate the coding regions of the basic and leucine zipper domains, respectively, in human XBP1 mRNA. The transcripts from the ERAI-LUC construct were not spliced under IRE1α-inactive conditions. The unspliced mRNA was translated into a truncated XBP1 protein with a FLAG tag at its amino terminus. Under IRE1α-active conditions, these transcripts were spliced, leading to a frame shift. The spliced mRNA was translated into an XBP1-luciferase fusion protein with a FLAG tag at its amino terminus. Thus, we detected luminescence only in IRE1α-active cells. (*B*) Northern blot analysis of *ERAI-LUC* transgene in embryos (E12.5), placentas (E12.5), and various tissues from adult wild-type and ERAI-LUC mice. Tg− and Tg+ indicate wild type and transgenic, respectively. Ethidium bromide staining (*Bottom*) shows the RNA loading control. (*C*) Bioluminescence imaging of liver, pancreas, and kidney tissues from adult wild-type and ERAI-LUC mice. The photo is a visible light image superimposed on an optical CCD bioluminescence image with a scale of photons per second per square centimeter per steradian (sr). Tunicamycin+ indicates i.p. injection with tunicamycin (500 ng/g body weight) 16 h before tissue collection. (*D*) Quantitative PCR analysis of endogenous *XBP1* in liver, pancreas, and kidney tissues of ERAI-LUC mice. Each sample is derived from tissues observed in *C*. Error bar indicates SEM ($n = 3$). From these data, we could confirm that the transgene was ubiquitously expressed in ERAI-LUC mice, the tissues of which emitted luminescence signals corresponding to the ER stress. This indicates that similar to the ERAI-GFP mouse, the ERAI-LUC mouse is a useful model for monitoring ER stress and IRE1α activity in vivo.

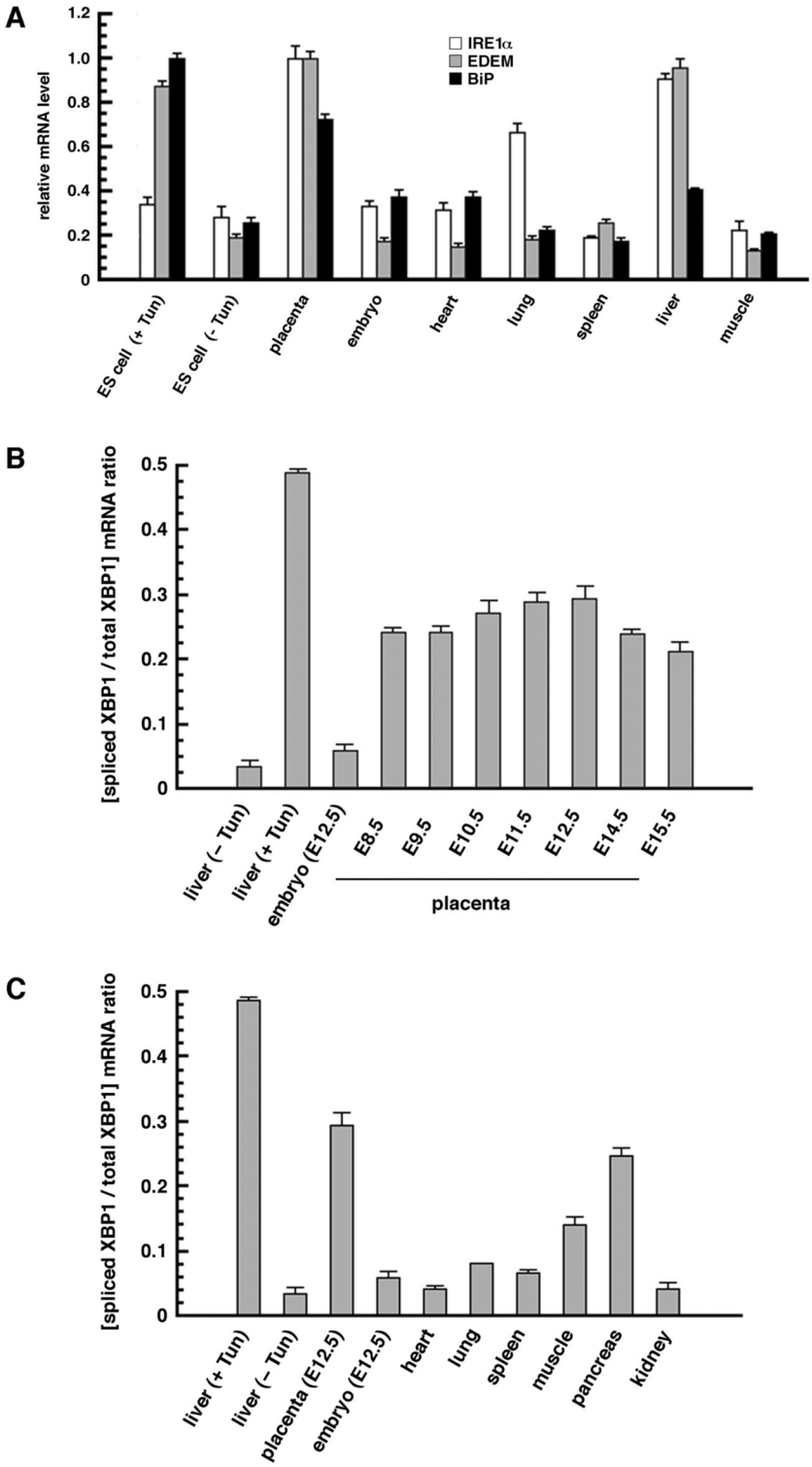

Fig. S2. Quantitative PCR analysis. (*A*) Quantitative PCR analysis of *IRE1α*, *EDEM*, and *BiP* in embryo (E11.5), placenta (E11.5), and various tissues of the adult wild-type mouse. +Tun and −Tun indicate treatment with and without 2 μg/mL tunicamycin (ER stressor) for 6 h, respectively. ES cells treated with or without tunicamycin were used as ER stress-induced or uninduced control samples, respectively. (*B*) Quantitative PCR analysis of *XBP1* in embryos and placentas. +Tun indicates i.p. injection with tunicamycin (500 ng/g body weight) 16 before tissue collection. Liver tissues of adult wild-type mice injected with or without tunicamycin were used as ER stress-induced or uninduced control samples, respectively. (*C*) Quantitative PCR analysis of *XBP1* in adult mouse tissues under physiological conditions. Liver tissues with tunicamycin were used as ER stress-induced control samples. Data of embryonic and placental tissues were presented for comparison. Error bar indicates SEM ($n = 3$).

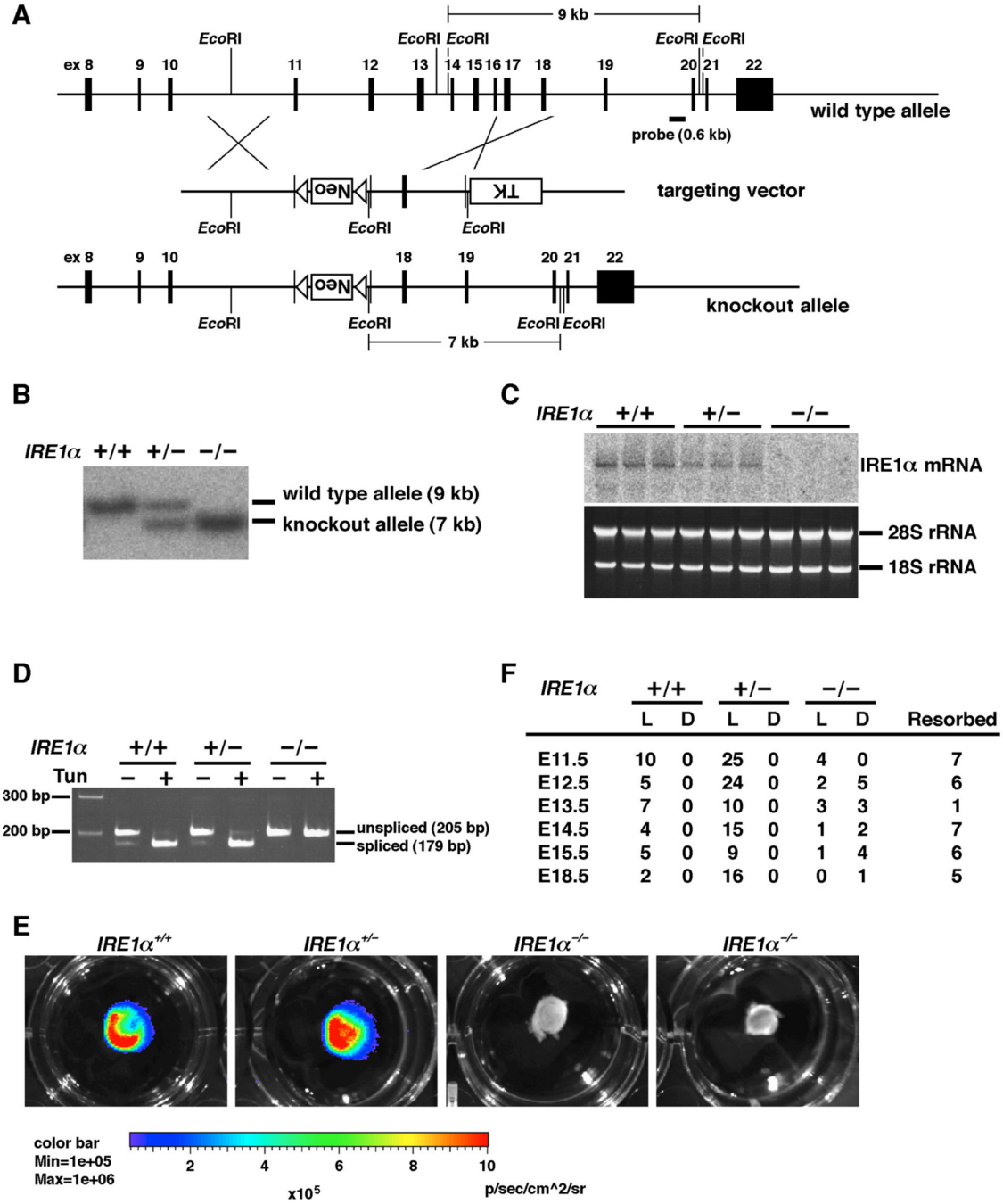

Fig. S3. Basic characterization of *IRE1α* conventional knockout mice. (*A*) Schematic diagram showing the predicted recombination of the targeting vector and the mouse *IRE1α* locus. Neo and TK indicate expression units of the neomycin resistance gene and thymidine kinase gene for positive and negative selections, respectively. (*B*) Southern blot analysis of offspring obtained from mating *IRE1α*$^{+/-}$ mice. (*C*) Northern blot analysis of *IRE1α* in *IRE1α*$^{+/+}$, *IRE1α*$^{+/-}$, and *IRE1α*$^{-/-}$ MEFs. Ethidium bromide staining (*Bottom*) shows the RNA loading control. (*D*) RT-PCR analysis of *XBP1* in *IRE1α*$^{+/+}$, *IRE1α*$^{+/-}$, and *IRE1α*$^{-/-}$ MEFs. +Tun and −Tun indicate treatment with and without 2 μg/mL tunicamycin for 6 h, respectively. (*E*) Bioluminescence imaging of the placentas of littermates obtained from mating a female *ERAI-LUC*$^{-/-}$; *IRE1α*$^{+/-}$ mouse and a male *ERAI-LUC*$^{+/+}$; *IRE1α*$^{+/-}$ mouse. The photos are a visible light image superimposed on an optical CCD bioluminescence image with a scale of photons per second per square centimeter per steradian (sr). (*F*) Number of embryos obtained from mating *IRE1α*$^{+/-}$ mice. L, live embryos; D, dead embryos. The viability of embryos was judged from their beating heart. From these data, we confirmed that exons 11–17 were deleted in the *IRE1α* knockout allele, that XBP1 splicing activity was lost in our *IRE1α*$^{-/-}$ mouse embryos similarly to the result in the previously reported *IRE1α* KO mouse, and that the embryos began to die at E12.5. We, however, used live embryos for examining *IRE1α*$^{-/-}$ mouse phenotypes at all analyzed stages to maximally exclude secondary effects due to the loss of IRE1α.

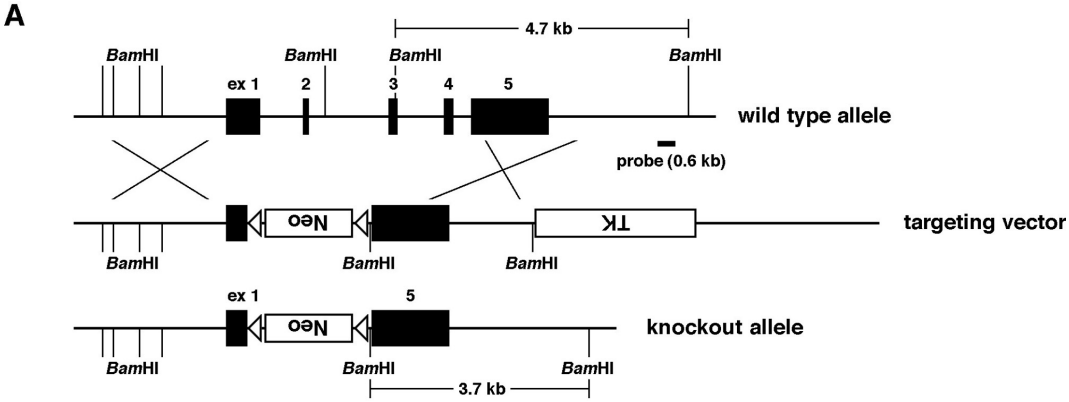

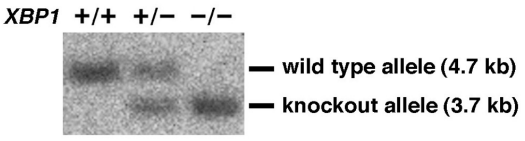

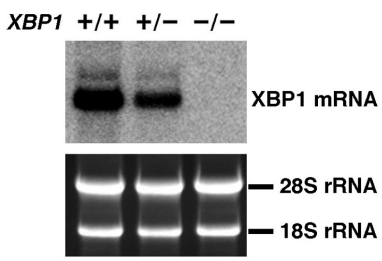

D

XBP1	+/+		+/−		−/−		
	L	D	L	D	L	D	Resorbed
E11.5	15	0	34	0	16	0	1
E12.5	13	0	26	0	14	0	10
E14.5	14	0	24	0	3	3	4

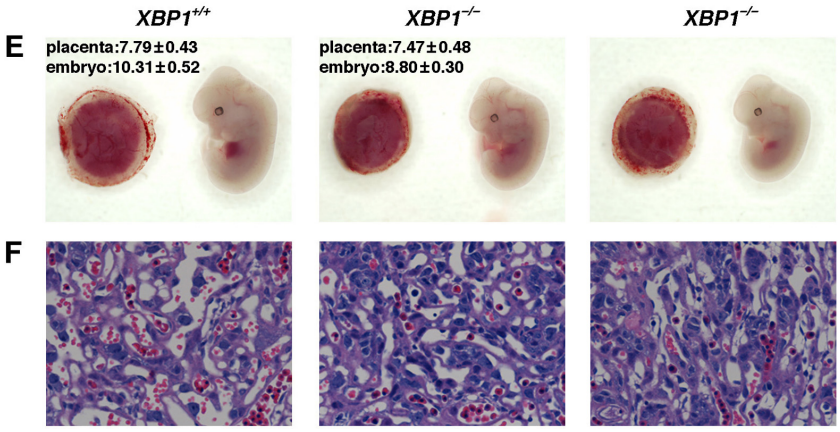

Fig. S4. Basic characterization of *XBP1* conventional knockout mice. (*A*) Schematic diagram showing the predicted recombination of the targeting vector and the mouse *XBP1* locus. ''Neo'' and ''TK'' indicate expression units of the neomycin resistance gene and thymidine kinase gene for positive and negative selections, respectively. (*B*) Southern blot analysis of offspring obtained from mating $XBP1^{+/-}$ mice. (*C*) Northern blot analysis of *XBP1* in $XBP1^{+/+}$, $XBP1^{+/-}$, and $XBP1^{-/-}$ MEFs. Ethidium bromide staining (bottom panels) shows the RNA loading control. (*D*) Number of embryos obtained from mating $XBP1^{+/-}$ mice. L, live embryos; D, dead embryos. The viability of embryos was judged from their beating heart. (*E*) Gross morphology of E13.5 wild-type ($XBP1^{+/+}$) and mutant ($XBP1^{-/-}$) embryos and placentas. Each number indicates the body length of embryo and the diameter of placenta (millimeter) as mean ± SD ($n = 11$). (*F*) H&E-stained E13.5 placental sections showing a region of the labyrinth layer in the placenta. (Original magnifications: *E*, 1×; and *F*, 20×.) From these data, we confirmed that exons 2–4 were deleted in the *XBP1* knockout allele, that *XBP1* KO mice died at the embryonic stage similarly to the results obtained in a previous report, that morphological and histological phenotypes in the placenta of *XBP1*-deficient mice were mild compared with those in the placenta of *IRE1*α-deficient mice, and that all examined *XBP1*-deficient mice survived until E12.5, although *IRE1*α-deficient mice began to die at E12.5.

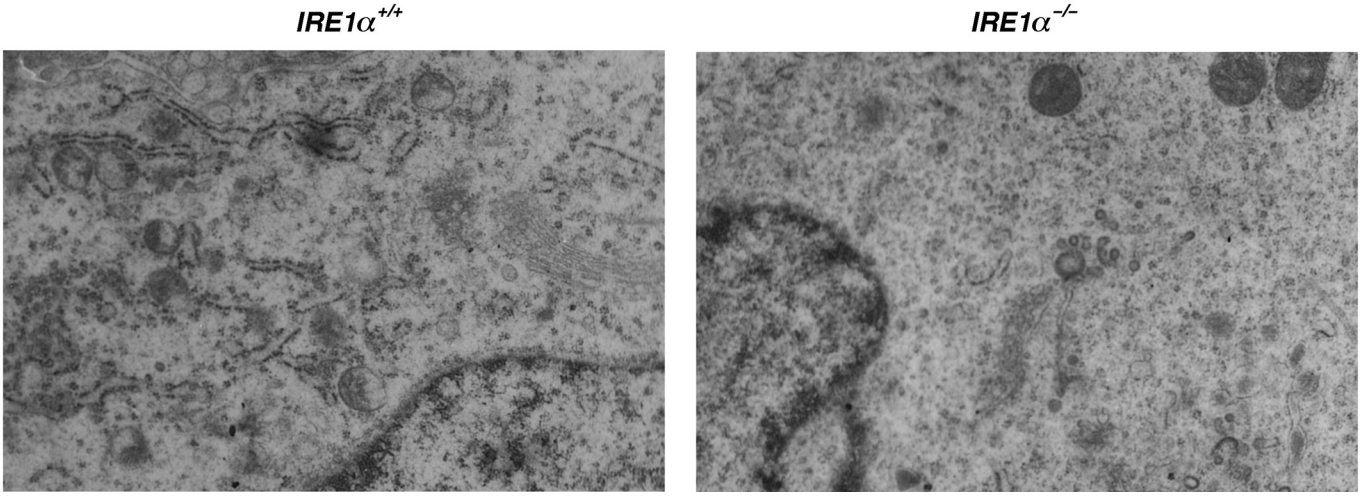

Fig. S5. Fig. 2*G* is enlarged for the presentation of fine subcellular structures.

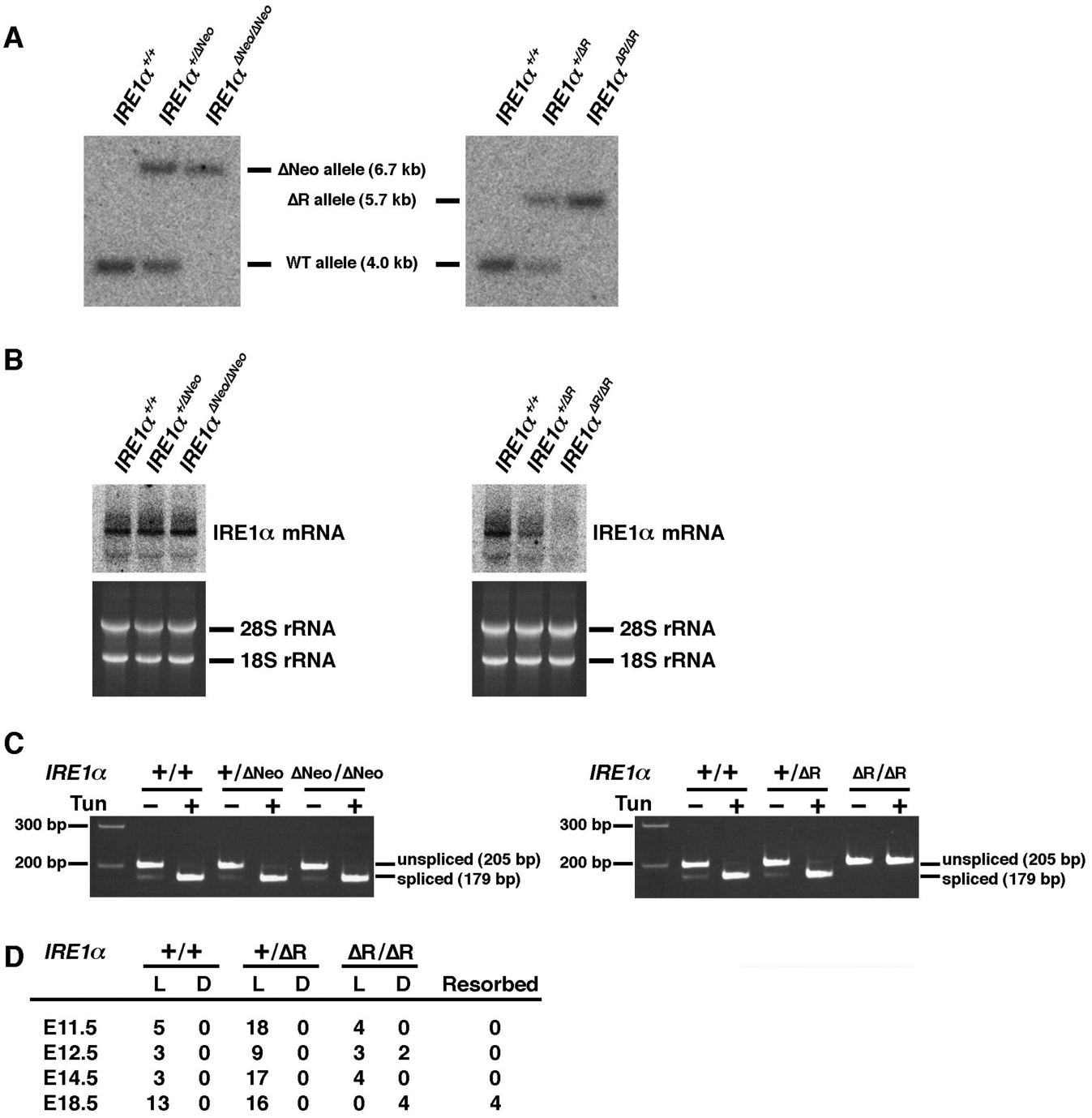

D

IRE1α	+/+		+/ΔR		ΔR/ΔR		
	L	D	L	D	L	D	Resorbed
E11.5	5	0	18	0	4	0	0
E12.5	3	0	9	0	3	2	0
E14.5	3	0	17	0	4	0	0
E18.5	13	0	16	0	0	4	4

Fig. S6. Basic characterization of *IRE1α* conditional knockout mice. (*A*) Southern blot analysis of offspring obtained from mating *IRE1α*$^{+/\Delta Neo}$ mice and from mating *IRE1α*$^{+/\Delta R}$ mice. (*B*) Northern blot analysis of *IRE1α* in *IRE1α*$^{+/+}$, *IRE1α*$^{+/\Delta Neo}$, *IRE1α*$^{\Delta Neo/\Delta Neo}$, *IRE1α*$^{+/\Delta R}$, and *IRE1α*$^{\Delta R/\Delta R}$ MEFs. Ethidium bromide staining (*Bottom*) shows the RNA loading control. (*C*) RT-PCR analysis of *XBP1* in *IRE1α*$^{+/+}$, *IRE1α*$^{+/\Delta Neo}$, *IRE1α*$^{\Delta Neo/\Delta Neo}$, *IRE1α*$^{+/\Delta R}$, and *IRE1α*$^{\Delta R/\Delta R}$ MEFs. +Tun and −Tun indicate treatment with and without 2 μg/mL tunicamycin for 6 h, respectively. (*D*) Number of embryos obtained from mating *IRE1α*$^{+/\Delta R}$ mice. L, live embryos; D, dead embryos. The viability of embryos was judged from their beating heart. From these data, we confirmed the deletion of exons 20–21 in the ΔR allele, although the ΔNeo allele of *IRE1α* was expressed normally. We also confirmed that *IRE1α*$^{\Delta R/\Delta R}$ mice obtained from mating *IRE1α*$^{+/\Delta R}$ mice lost XBP1 splicing activity and began to die at E12.5, similarly to *IRE1α*$^{-/-}$ mice, whereas *IRE1α*$^{\Delta Neo/\Delta Neo}$ mice obtained from mating *IRE1α*$^{+/\Delta Neo}$ mice retained XBP1 splicing activity, and they grew and bred normally.

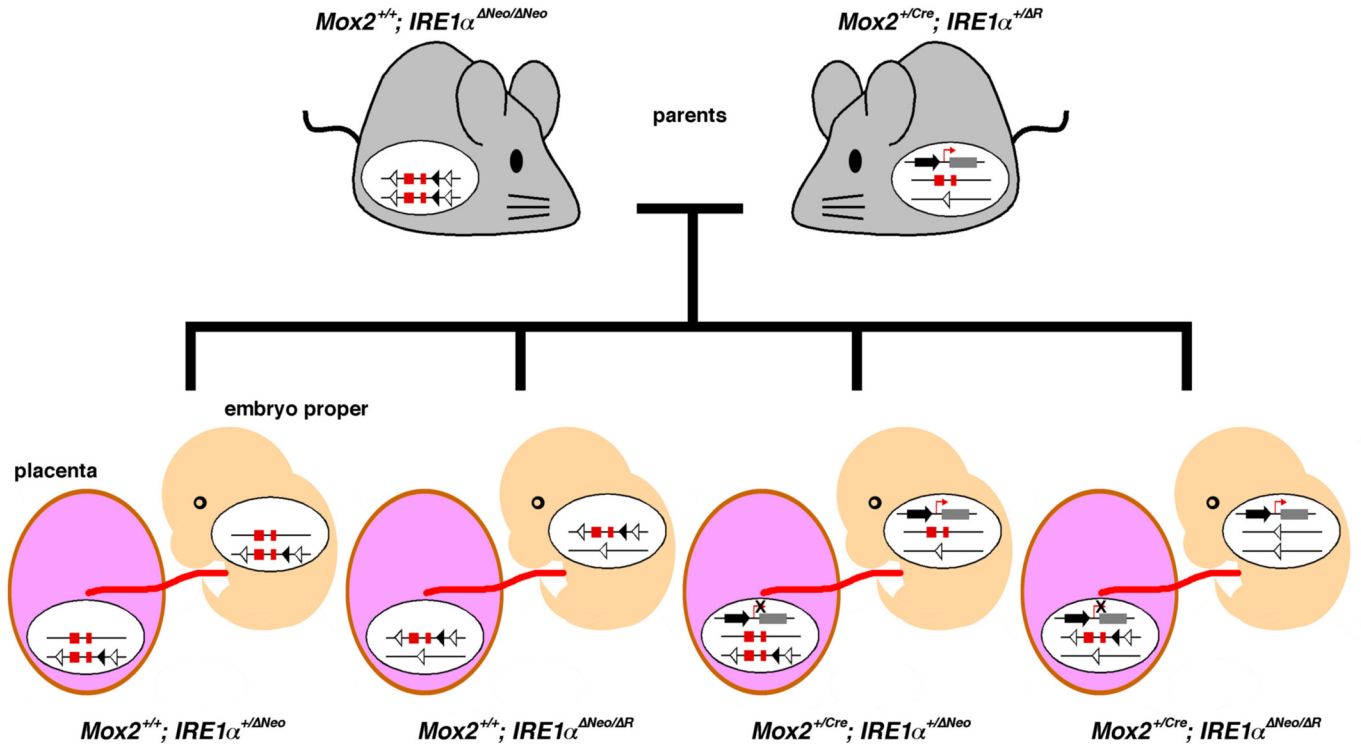

Fig. S7. The genotype of mice generated by breeding *Mox2*$^{+/Cre}$; *IRE1*$\alpha^{+/\Delta R}$ mice with *IRE1*$\alpha^{\Delta Neo/\Delta Neo}$ mice. Schematic diagram shows parental, fetal, and placental genotype. Black arrow, *Mox2* promoter; gray box, *Cre*; red boxes, exons 20–21 of *IRE1*α; closed arrowhead, FRT element; open arrowhead; loxP element. X symbol indicates repression of *Mox2* promoter activity in the placenta. The ΔNeo alleles in *Mox2*$^{+/Cre}$; *IRE1*$\alpha^{+/\Delta Neo}$ embryo proper and *Mox2*$^{+/Cre}$; *IRE1*$\alpha^{\Delta Neo/\Delta R}$ embryo proper were changed into the ΔR alleles by Cre recombinase. Thus, *Mox2*$^{+/Cre}$; *IRE1*$\alpha^{\Delta Neo/\Delta R}$ embryo proper was of *IRE1*α-deficient type.

Table S1. Essential fatty acid transport in *IRE1α*-deficient placentas

	Placenta			Fetus		
Fatty acid	*IRE1*$\alpha^{+/+}$, μg/g tissue weight	*IRE1*$\alpha^{-/-}$, μg/g tissue weight	Reduction, %	*IRE1*$\alpha^{+/+}$, μg/g tissue weight	*IRE1*$\alpha^{-/-}$, μg/g tissue weight	Reduction, %
Palmitic acid	2,480.0 ± 440.3	2,295.3 ± 166.5	7.4	1,858.4 ± 172.7	1,788.2 ± 223.6	3.8
Stearic acid	2,547.2 ± 496.9	2,481.2 ± 194.4	2.6	845.0 ± 79.3	789.9 ± 70.0	6.5
Linoleic acid*	1,290.4 ± 244.1	1,251.6 ± 92.5	3.0	276.2 ± 33.5	170.1 ± 17.7	38.4
Arachidonic acid*	1,683.0 ± 256.6	1,605.3 ± 111.1	4.6	703.5 ± 58.7	594.8 ± 53.1	15.4
Docosahexaenoic acid*	1,039.1 ± 212.9	1,029.2 ± 63.9	1.0	383.0 ± 39.6	296.1 ± 19.8	22.7

The quantity of each fatty acid is presented as mean ± SD ($n = 8$).
Reduction is a value calculated by using the following formula: ([mean of *IRE1*$\alpha^{+/+}$] − [mean of *IRE1*$\alpha^{-/-}$])/([mean of *IRE1*$\alpha^{+/+}$] × 100).
*Essential fatty acid.

Table S2. Primer information

Name	Sequence
5′ primer for 5′ IRE1α homology arm	5′-cggggtacccttgttatttccactctataagaatactgg-3′
3′ primer for 5′ IRE1α homology arm	5′-ccgctcgagagacagaggagtttcatggtgtcc-3′
5′ primer for 3′ IRE1α homology arm	5′-ccggaattcccagagatgctgagtgaagactgtaaggacaacc-3′
3′ primer for 3′ IRE1α homology arm	5′-ccggaattcctctatcaattcacgagcaatgacgtcc-3′
5′ primer for 5′ XBP1 homology arm	5′-cggggtacctcaaagagccaatctgaacc-3′
3′ primer for 5′ XBP1 homology arm	5′-ccgctcgagccatagccaggaaacgtctacg-3′
5′ primer for 3′ XBP1 homology arm	5′-cggggtaccggatccgtcgaccctgtgatctgagagtgtaagc-3′
3′ primer for 3′ XBP1 homology arm	5′-ccgctcgagggatcccgtgactgctgtctagctccagc-3′
5′ primer for 5′ CKO homology arm	5′-ccggaattcgtcgacgtctagtcatgaccatctacacactgg-3′
3′ primer for 5′ CKO homology arm	5′-ggaagatctgcggccgcctcgagtagccagaaggtcatacgcctcacttgagc-3′
5′ primer for conditional targeting region	5′-cggggtaccaagcttatcgattgaggaacctgcagcctagacc-3′
3′ primer for conditional targeting region	5′-ccgctcgagaagcttcataagccatcaatctctgc-3′
5′ primer for 3′ CKO homology arm	5′-ccggaattcagatctatcgattttaactggaagcttgcttacagttctagagg-3′
3′ primer for 3′ CKO homology arm	5′-ccgctcgagagatcttcacattggtcttggctgttacctctcagc-3′